Path Loss at 5 GHz and 31 GHz for Two Distinct Indoor Airport Settings

David W. Matolak
Dept. of Electrical Engineering
University of South Carolina
Columbia, SC, USA
matolak@sc.edu

Mohanad Mohsen
Dept. of Electrical Engineering
University of South Carolina
Columbia, SC, USA
mmohsen@email.sc.edu

Jinming Chen
School of Information & Comm. Eng.
Univ. Electronic Science and Technology
Chengdu, China
jeremychen1881@gmail.com

***Abstract*—Vehicular and indoor communications continue to grow. This pertains to applications in aviation as well, which is also experiencing rapid growth. Since a pre-requisite to reliable communication link design is accurate knowledge of the wireless channel, research on channel models for these environments is an active area of study, and this is the topic of this paper. In this work, we report on measurement and model results for propagation path loss in two indoor airport environments, in two frequency bands. The first environment is a typical small terminal building, with characteristics similar to indoor offices, and the second is a more unusual aircraft maintenance hangar. The hangar is a crowded environment with multiple aircraft and metallic objects. Our results are for both the 30 GHz band (specifically 31 GHz), which is being investigated for future 5th generation cellular and other applications, and for the 5 GHz band, for a comparison. Our results show that the airport terminal building exhibits path loss characteristics very similar to those of an indoor office environment, at both frequencies, and this is largely as expected. In contrast, the maintenance hangar path loss is less than that of non-line of sight terminal building regions, somewhat unexpectedly. We attribute this to the highly reflective hangar environment, which serves to compensate for reduced diffraction and increased blockage losses at 31 GHz.**

Keywords—propagation, wireless channel, millimeter wave

I. Introduction

Communication systems for vehicles have seen rapid growth in recent years, e.g., [1]. We specifically refer to terrestrial communication systems dedicated to links between vehicles, termed vehicle-to-vehicle (V2V), as well as communication between vehicles and infrastructure (V2I). These cases are distinct from those using other established infrastructure such as cellular and broadcast radio. The majority of V2V/V2I research and development pertains to established roadways, although "off-road" V2V communications will also be of interest. The set of mobile platforms that inter-communicate will also be generalized in the future to encompass V2V communications among watercraft (both on and below the surface), aircraft, underground vehicles, and spacecraft.

The rise in use of robotics also means that many vehicles will be autonomous, or self-guided (unmanned is the typical term when describing aircraft). Many such robotic vehicles will operate indoors [2], and this motivates the work here, where we consider communications in two airport environments.

All modern wireless communication system standardization begins with a characterization of the wireless channel over which the system will operate, and V2V channels are no exception [3]-[6]. The recent rise in the use of unmanned aerial vehicles (UAVs), also known as drones, has elicited much work on air-ground (AG) channel characterization, for example [7].

In our current project with NASA, we are investigating new communication solutions for aviation [8]. This includes AG and air-air (AA) communication, as well as communication at airports. Since airports can be thought of as hubs of the air traffic management (ATM) system, their efficiency is critical to efficient ATM. This airport communication includes both outdoor communication with aircraft, airport surface vehicles, airport security, etc., as well as indoor communication within airport buildings, including terminal buildings, offices, storage facilities and hangars, and maintenance buildings.

In one portion of our work we are studying the potential use of millimeter wave (mmWave) frequency bands for short range communications. This is a very active area for 5th-generation (5G) cellular [9]-[11]. In our work we are considering mmWave bands for short range V2V links, as well as for V2I and fixed links in airport areas. Frequency bands we are addressing are 30 GHz, 60 GHz, and 90 GHz, and in this paper we report on airport channel measurements at 30 GHz; little has appeared on this in the literature. We also note that our actual center frequency was 31 GHz, but since these wavelengths are essentially the same for propagation purposes, there will be no statistical differences between results for 30 and 31 GHz; hence we refer to both 30 and 31 GHz synonymously. We also made measurements at 5 GHz for comparison purposes.

The measurements were of propagation path loss, vital for link budget and coverage analyses. There is a growing amount of results for path loss in the 30 GHz band and in bands close to this, e.g., the 28 GHz band [11], and we compare our results to these for the rather unique airport environments.

The remainder of this paper is organized as follows: in Section II we describe the indoor airport environments in which we made our path loss measurements. Section III briefly summarizes our test equipment and the path loss measurement procedures. In Section IV we provide the path loss results and models, and Section V concludes the paper.

This work was sponsored by NASA, award NNX17AJ94A.

978-9-0827-9703-9/19/$31.00 ©2019 IEEE

II. Environment Descriptions

Our measurement environments were both indoors. The airport is a small municipal airport in Columbia, SC, USA, the Jim Hamilton L. B. Owens Airport, with airport designator CUB. Measurements were made in the small airport terminal building and in the nearby aircraft maintenance hangar.

A. Airport Terminal Building

The airport terminal building is a small office-type building with a customer service area, a hallway with offices on both sides, and a small second-floor office area over the western portion of the building. Our measurements here pertain to the first floor, whose plan appears in Fig. 1. Photos of the measurement areas from the perspective of the transmitter location appear in Fig. 2.

The terminal building exhibits typical indoor office characteristics, with tiled and carpeted floors, plasterboard walls, large windows, and acoustic tile dropped ceilings. Measurements were made for three line of sight (LOS) paths, and a set of non-LOS (NLOS) locations. The transmitter (Tx) was kept fixed near a corner of the open customer service area. Link distances reached up to approximately 20 m, and the environment was largely time invariant during measurements.

B. Airport Maintenance Hangar

The maintenance hangar is a metal building, with an approximate 30 by 40 m footprint, with interior thermal insulation (foil-backed), open from concrete floor to its ceiling of height approximately 10 m. The hangar contained six or seven small-medium aircraft, plus large metal tool chests, tables of various sizes, metal and plastic cabinets, etc. Figure 3 shows a photo with one of the hangar bay doors open. Measurements were made during normal work hours, with the bay doors closed except for a very brief period. During the measurement time, the airport maintenance team personnel moved about occasionally. A few tool cabinets and tables were also moved over the course of the measurement period of approximately 4 hours, but as with the terminal building, the channel was time invariant during measurements.

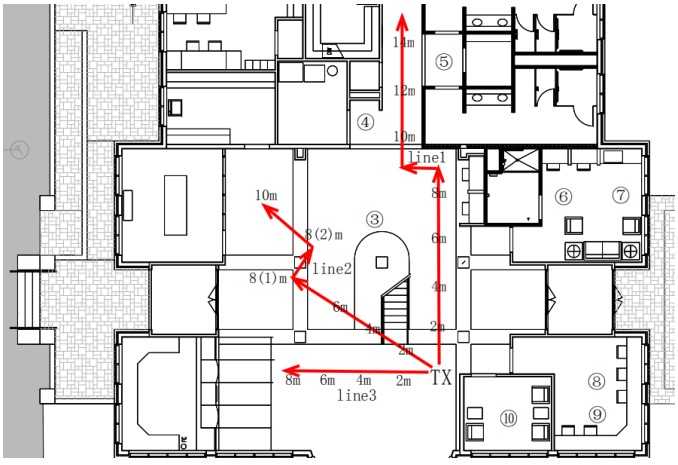

Fig. 1. Floor plan of 1st floor of CUB terminal building, showing transmitter (Tx) location and receiver (Rx) paths designated by red lines (LOS locations), with several NLOS locations indicated by numbered circles.

Fig. 2. Photographs of 1st floor of CUB terminal building, showing LOS receiver (Rx) travel paths from transmitter (Tx) perspective.

In this atypical setting, it was difficult to ensure long paths of continuous LOS or NLOS conditions without artificially configuring local obstacles (some of which was impossible, e.g., moving aircraft). Thus our maintenance hangar results are reported as a mixture of LOS and NLOS conditions. Although this may be unusual, it is quite practical for such an environment where local obstacles will move during the day. As will be shown, LOS conditions pertain mostly for the shortest distances.

III. Equipment and Measurement Procedures

For the 31 GHz measurements, we used a Rohde and Schwarz (R&S) dual RF output vector signal generator (VSG), model SMW 200A as transmitter, and an R&S signal and spectrum analyzer, model FSW 43, as receiver. At the transmitter, a R&S 5 GHz CW signal was upconverted using a Microwave Dynamics (MD) LO-MIX301-2832 upconverter, followed by an MD2832 power amplifier. Transmitted power to the Pasternack model PE9850/2F-10 horn antenna was approximately 26.5 dBm. The 31 GHz antenna had gain 10 dB, and beamwidth 54 degrees. The same type of antenna was used at the receiver. No Rx downconverter was required, as the R&S FSW has an upper frequency limit of 43 GHz. Both Tx and Rx were placed atop equipment carts. Figure 4 shows the test setup.

Fig. 3. Photograph of CUB maintenance hangar, showing several transmitter (Tx) locations and receiver (Rx) paths.

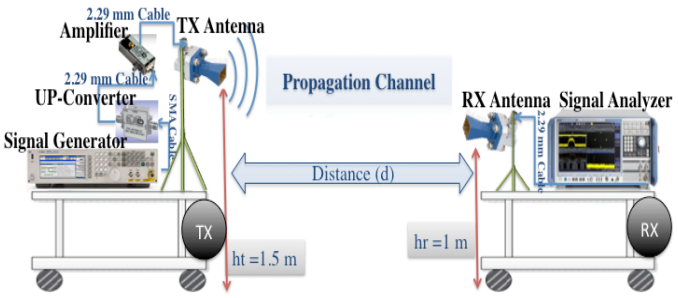

Fig. 4. Diagram of 30 GHz measurement setup.

The 5 GHz measurements also used a CW signal: the transmitter was the second RF output port of the R&S VSG, set to send a 19 dBm sinusoid into an omnidirectional monopole antenna model HGV-4958-06U, manufactured by L-com Global Connectivity, with approximately 6 dB gain. The 5 GHz receiver was an Agilent portable spectrum analyzer, model N9342C, and used the same type of antenna as the transmitter.

For measurement procedures, once the transmitters were configured to transmit, the receivers (both on the same cart) were moved to the Rx locations described in the prior section. At each location, three measurements, separated by at least one-half wavelength, were made of the received signal strength. These measurements were then used, along with knowledge of transmitter power and cable losses, to compute the estimated path loss L in dB:

$$P_r = P_t + G_t + G_r - L_c - L \qquad (1)$$

where P_t is transmit power in dBm, P_r is received power in dBm, G_t and G_r are the transmitter and receiver antenna gains in dB, respectively, and L_c is the combined cable loss in dB at Tx and Rx. Distance was measured with a laser rangefinder and checked with a measuring tape, yielding distance accuracy on the order of a few cm.

For the directional 31 GHz measurements, we approximately aligned the Tx and Rx antenna boresights at each location, including the NLOS locations. Hence we did not attempt to scan then aim the Rx or Tx antennas to maximize received power via a strong reflection. The idea was to not presume use of antenna adaptation to minimize path loss, but rather assess average loss with these modest antenna beamwidths and with a coarse alignment procedure suitable for non-expert installations. This is also suitable for such an environment as the hangar, where obstacles such as aircraft and equipment will often be moved from day to day. All antennas used vertical polarization.

IV. Path Loss Results and Models

Two types of models [11] were fit to the data: the close-in (CI) reference distance model, with free-space attenuation reference distance of d_0=1 m, and the floating-intercept (FI) model. The CI and FI path loss models are given as

$$L_{CI}(d) = L_{FS}(d_0) + 10n\log(d/d_0) + X_{CI}, \qquad (2)$$

$$L_{FI}(d) = \alpha + 10\beta\log(d) + X_{FI}. \qquad (3)$$

where both losses are in dB, $L_{FS}(d_0)$ is the free-space path loss in dB at the reference distance ($20\log(4\pi d_0/\lambda)$, with λ=wavelength), the floating intercept α is in dB, n and β are dimensionless slopes on the log-log scale, and the X's are the random variables quantifying the goodness of the model fits. For NLOS cases, X represents so-called shadowing, typically modeled as a zero-mean Gaussian random variable, with standard deviation σ. Although both models are used by researchers, the CI form appears to be becoming the more widely accepted. Hence even though we provide parameters for both FI and CI models, most of our discussion focuses on the CI models. The CI model parameters for all cases appear in Table I; the FI parameters are provided only in the figure legends.

A. Terminal Building

Plots of terminal building path loss in dB vs. link distance in meters appear in Figures 5 and 6, for the 5 GHz and 31 GHz frequencies, respectively. Figures 5 and 6 also show dashed (CI) lines with path loss exponent (n) values from 1-4, as reference slope values; the free-space path loss line is that for n=2.

The LOS path loss exponents n and β are very close to the free space value of 2 for 31 GHz, but the CI 5 GHz LOS exponent n~3 is unusual; we are still investigating the cause of this. The CI NLOS exponents are as expected larger than those for the LOS case, equal to 3.2 for 5 GHz and 4.5 for 31 GHz. Larger penetration losses through walls contribute to the larger 31 GHz slope. All LOS standard deviations σ<3 dB. Compared with results for 28 GHz in [11], the airport terminal building 31 GHz path loss parameters n and σ are all very comparable.

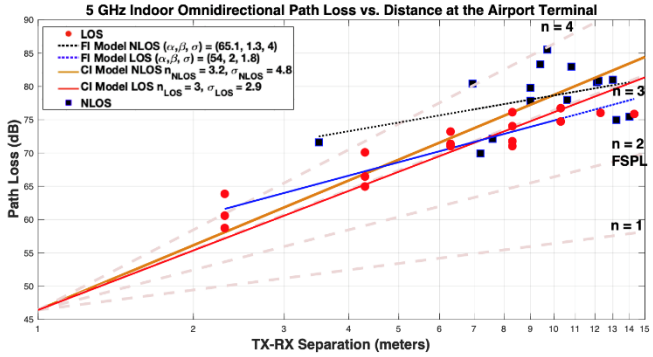

Fig. 5. Plot of 5 GHz path loss vs. distance. Measured data represented by symbols, CI fits in solid lines with intercept at 1 m, and FI fits in dotted lines.

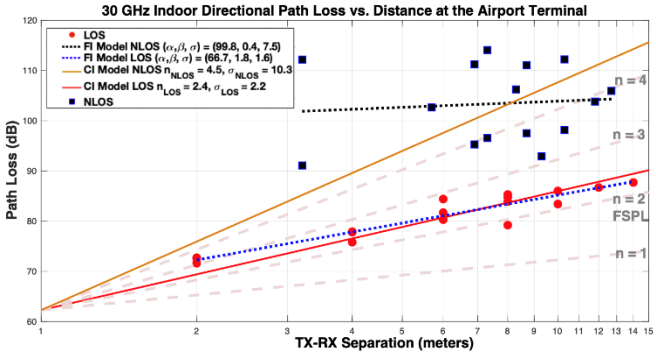

Fig. 6. Plot of 30 GHz path loss vs. distance. Measured data represented by symbols, CI fits in solid lines with intercept at 1 m, and FI fits in dotted lines.

B. *Maintenance Hangar*

In the maintenance hangar we employed two Tx locations and a total of five Rx paths. As noted, we report results for LOS and NLOS conditions together, since in this rather cluttered environment, finding specific LOS and NLOS paths would be rather artificial. Figure 7 shows results for just the first "run" (Rx line) for the first Tx location, for both frequencies. Figure 8 shows the combined results of all three runs for Tx location 1. The abbreviation "OLOS" in the legends stands for obstructed LOS data, indicating only a partial obstruction of the LOS between the antennas.

The larger data set in Fig. 8 yields a smaller σ than for the individual run of Fig. 7, as expected, but otherwise, all three run model parameters are close to the average. The NLOS locations typically only occur beyond a minimum distance of approximately 8 m for this Tx location, whereas LOS locations occur throughout the run. Figure 9 shows results for the second Tx location, with comparable results, and slightly smaller values of σ than for Tx location 1.

Figure 10 shows results for all maintenance hangar data. The 31 GHz FI and CI models have nearly identical parameters in this case, with path loss exponents just less than three. The omnidirectional 5 GHz results have a similar path loss exponent, but smaller σ. Ultimately the larger σ at 31 GHz is likely attributable to the reduced diffraction and increased blockage attenuation relative to 5 GHz.

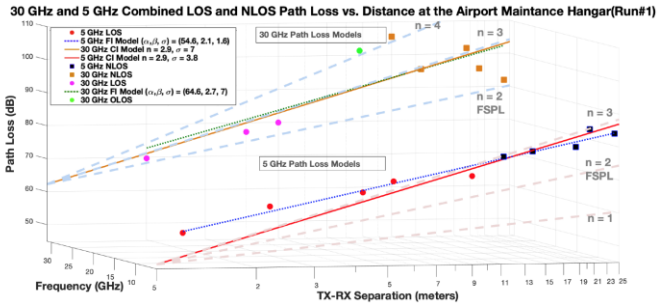

Fig. 7. Plot of 30 GHz and 5 GHz path loss vs. distance for run 1, Tx location 1. Measured data represented by symbols, CI fits in solid lines with intercept at 1 m, and FI fits in dotted lines.

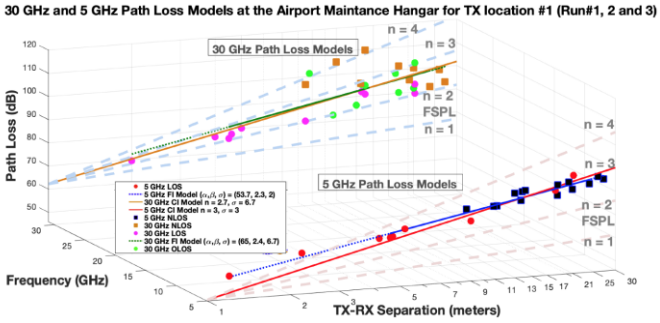

Fig. 8. Plot of 30 GHz and 5 GHz path losses vs. distance for all three runs for Tx location 1. Measured data represented by symbols, CI fits in solid lines with intercept at 1 m, and FI fits in dotted lines.

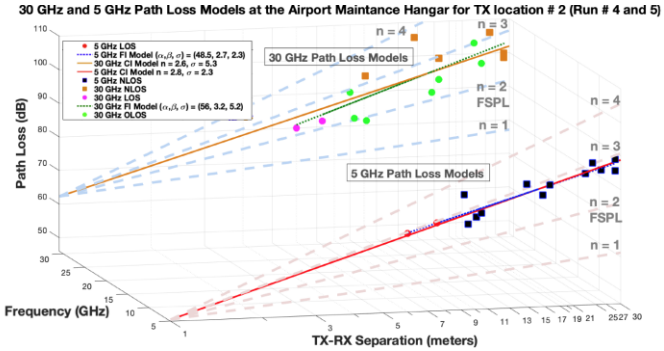

Fig. 9. Plot of 30 GHz and 5 GHz path losses vs. distance for both runs for Tx location 2. Measured data represented by symbols, CI fits in solid lines with intercept at 1 m, and FI fits in dotted lines.

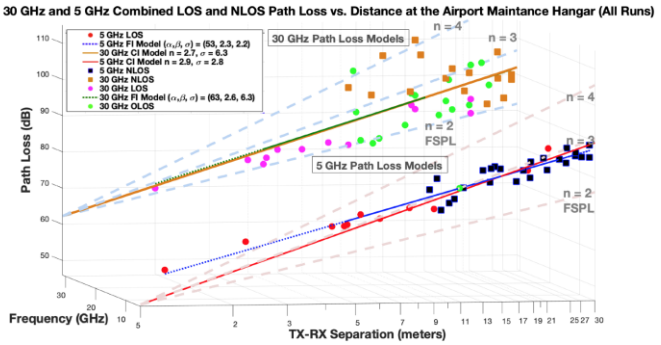

Fig. 10. Plot of 30 GHz and 5 GHz path losses vs. distance for all runs for all Tx locations. Measured data represented by symbols, CI fits in solid lines with intercept at 1 m, and FI fits in dotted lines.

For individual runs within the maintenance hangar, some variation occurs for the mmWave results, e.g., σ ranges from 3.6-7 dB. We also note that excluding the short-range LOS points from the model fits changes σ only slightly, e.g., increasing it by ~0.5 dB. Overall, for 31 GHz, the fairly rich-scattering maintenance hangar environment provides a *smaller* path loss exponent and *smaller* spread σabout the fit than the typical office environment's NLOS regions.

TABLE I. CI PATH LOSS MODEL PARAMETERS

	n	**σ**
	Terminal Building	
5 GHz LOS	3	2.9
5 GHz NLOS	3.2	4.8
31 GHz LOS	2.4	2.2
31 GHz NLOS	4.5	10.3
	Maintenance Hangar	
5 GHz Mixed	2.9	2.8
31 GHz Mixed	2.7	6.3

V. CONCLUSION

To plan for the growth in vehicular communications, both outdoors and indoors, new communication systems are being researched. For these new systems, some of which will be deployed in the mmWave bands, accurate channel models are

needed, and in this paper we provided propagation path loss models in two frequency bands—5 GHz and 31 GHz—for two distinct indoor airport locations: a small terminal building, and an aircraft maintenance hangar. We found the airport terminal building results to closely follow those found by other researchers for indoor office environments: LOS path loss exponents are near the free-space value of two, and standard deviations are a few dB, and NLOS path loss exponents are larger (~3-4), with larger standard deviations as well. The maintenance hangar is an atypical environment, with many large and small metallic obstacles, as well as foil-insulation-lined metal walls. Since these objects are frequently moved, e.g., hourly, we made no attempt to artificially separate LOS from NLOS conditions, and hence report path loss results for these mixed conditions. In the hangar, for both frequency bands, path loss exponents are near three, and standard deviations are only 2.8 dB for 5 GHz, and 6.3 dB for 31 GHz. These smaller than expected standard deviations likely arise from the rich scattering environment, yielding less variation than the NLOS indoor office settings. Future work includes additional measurements at another mmWave frequency (90 GHz) as well as wideband measurements for channel impulse response estimation.

ACKNOWLEDGMENT

For assistance with measurements, the authors would like to thank H. Jamal, J. Liu, N. Hosseini, A. Grant, H. K. McGill, and H. E. King of the University of South Carolina. The authors would also like to thank C. S. Eversmann, and F. Schumpert of the Jim Hamilton—L. B. Owens Airport for their support with airport access.

REFERENCES

[1] ETSI, "Intelligent Transport Systems (ITS); European profile standard on the physical and medium access layer of 5 GHz ITS," *Draft ETSI ES, vol. 202, no. 663, p. V0*, 2009.

[2] T. Deyle, "Why indoor robots for commercial spaces are the next big thing in robotics," *IEEE Spectrum*, May 2017.

[3] I. Sen, D. W. Matolak, "Vehicle-vehicle channel models for the 5 GHz band," *IEEE Trans. Intelligent Transportation Systems*, vol. 9, no. 2, pp. 235-245, June 2008.

[4] A. Molisch, F. Tufvesson, J. Karedal, C. Mecklenbräuker, "A survey on vehicle-to-vehicle propagation channels," *IEEE Wireless Comm. Mag.*, vol. 16, no. 6, pp. 12–22, 2009.

[5] Q. Wang, D. W. Matolak, B. Ai, "Shadowing characterization for 5 GHz vehicle-to-vehicle channels," *IEEE Vehicular Tech.,* vol. 67, no. 3, pp. 1855-1866, March 2018.

[6] IEEE Draft Standard for Information Technology—Telecommunications and Information Exchange Between Systems—Local and Metropolitan Area Networks—Specific Requirements—Part 11: Wireless LAN Medium Access Control (MAC) and Physical Layer (PHY) Specifications Amendment 7: Wireless Access in Vehicular Environments, *IEEE Unapproved Draft Std P802.11p /D7.0*, May 2009.

[7] D. W. Matolak, R. Sun, "Air-ground channel characterization for unmanned aircraft systems—part I: methods, measurements, and results for over-water settings," *IEEE Trans. Veh. Tech.*, vol. 66, no. 1, pp. 26-44, Jan. 2017.

[8] D. W. Matolak, I. Guvenc, H. Mehrpouyan, G. Carr, "Hyper-spectral communications, networking & ATM: progress and perspectives," *AIAA/IEEE DASC*, London, UK, 23-27 September 2018.

[9] P. Wang, Y. Li, L. Song, B. Vucetic, "Multi-gigabit millimeter wave wireless communications for 5G: from fixed access to cellular networks," *IEEE Comm. Mag*., vol. 53, no. 1, pp. 168-177, January 2015.

[10] H. Ji, S. Park, J. Yeo, Y. Kim, J. Lee, B. Shim, "Ultra-reliable low-latency communications in 5G downlink: physical layer aspects," *IEEE Wireless Comm. Mag*., vol. 25, no. 3, pp. 124-130, June 2018.

[11] G. R. Maccartney, T. S. Rappaport, S. Sun, S. Deng, "Indoor office wideband millimeter-wave propagation measurements and channel models at 28 and 73 GHz for ultra-dense 5G wireless networks," *IEEE Access,* vol. 3, pp. 2388–2424, 2015.